

INTRODUCTION

Forest insects and diseases have widespread ecological and economic impacts on the forests of the United States and may represent the most serious threats to the Nation's forests (Logan and others 2003, Lovett and others 2016, Tobin 2015). U.S. law therefore authorizes the U.S. Department of Agriculture Forest Service to “conduct surveys to detect and appraise insect infestations and disease conditions and man-made stresses affecting trees and establish a monitoring system throughout the forests of the United States to determine detrimental changes or improvements that occur over time, and report annually concerning such surveys and monitoring” (FHP 2020). Insects and diseases cause changes in forest structure and function, species succession, and biodiversity, which may be considered negative or positive depending on management objectives (Edmonds and others 2011). Nearly all native tree species of the United States are affected by at least one injury-causing insect or disease agent, with exotic agents on average considerably more severe than native ones (Potter and others 2019a). Additionally, the genetic integrity of several native tree species is highly vulnerable to exotic diseases and insects (Potter and others 2019b).

An important task for forest managers, pathologists, and entomologists is recognizing and distinguishing between natural and excessive mortality, a task that relates to ecologically based or commodity-based management objectives (Teale and Castello

2011). The impacts of insects and diseases on forests vary from natural thinning to extraordinary levels of tree mortality, but insects and diseases are not necessarily enemies of the forest because they kill trees (Teale and Castello 2011). If disturbances, including insects and diseases, are viewed in their full ecological context, then some amount can be considered “healthy” to sustain the structure of the forest (Manion 2003, Zhang and others 2011) by causing tree mortality that culls weak competitors and releases resources that are needed to support the growth of surviving trees (Teale and Castello 2011).

Analyzing patterns of forest insect infestations, disease occurrences, forest declines, and related biotic stress factors is necessary to monitor the health of forested ecosystems and their potential impacts on forest structure, composition, biodiversity, and species distributions (Castello and others 1995). In particular, introduced insects and diseases can extensively damage the biodiversity, ecology, and economy of affected areas (Brockerhoff and others 2006, Mack and others 2000). Few forests remain unaffected by invasive species, and their devastating impacts in forests are undeniable, including, in some cases, wholesale changes to the structure and function of an ecosystem (Parry and Teale 2011).

Examining insect pest occurrences and related stress factors from a landscape-scale perspective is useful, given the regional extent of many infestations and the large-scale complexity of interactions between host

CHAPTER 2.

Broad-Scale Patterns of Insect and Disease Activity across the 50 United States from the National Insect and Disease Survey, 2019

KEVIN M. POTTER
JEANINE L. PASCHKE
FRANK H. KOCH
ERIN M. BERRYMAN

distribution, stress factors, and the development of insect pest outbreaks (Holdenrieder and others 2004, Liebhold and others 2013). One such landscape-scale approach is detecting geographic patterns of disturbance, which allows for the identification of areas at greater risk of significant ecological and economic impacts and for the selection of locations for more intensive monitoring and analysis. National Insect and Disease Survey (IDS) data (FHP 2020), coordinated by the Forest Health Protection (FHP) program of the Forest Service, provide an important source of information about forest disturbances and their causal agents across broad regions. Recent long-term analyses of these data underscored that insects have been much more widespread agents of mortality than diseases, with bark beetles consistently the most important mortality agents across regions and over time (Potter and others 2020a). Additionally, the tree canopy area affected by nonnative invasive agents of mortality and defoliation has remained relatively consistent over time (with a larger relative impact on forests in the North), and tree canopy area affected by defoliation agents has usually exceeded or equaled the area affected by mortality agents (Potter and others 2020a).

METHODS

Data

National Insect and Disease Survey data (FHP 2020) consist of information from low-altitude aerial survey and ground survey efforts by FHP and partners in State agencies. These data can be used to identify forest landscape-scale patterns

associated with geographic hot spots of forest insect and disease activity in the conterminous 48 States (CONUS) and to summarize insect and disease activity by regions in the CONUS, Alaska, and Hawaii (Potter 2012, 2013; Potter and Koch 2012; Potter and Paschke 2013, 2014, 2015a, 2015b, 2016, 2017; Potter and others 2018, 2019c, 2020b).

The IDS data identify areas with mortality and defoliation caused by insect and disease activity, although some important forest insects (such as emerald ash borer [*Agrilus planipennis*] and hemlock woolly adelgid [*Adelges tsugae*]), diseases (such as laurel wilt [*Raffaelea lauricola*], Dutch elm disease [*Ophiostoma novo-ulmi*], white pine blister rust [*Cronartium ribicola*], and thousand cankers disease [*Geosmithia morbida*]), and mortality complexes (such as oak decline) are not easily detected or thoroughly quantified through aerial detection surveys. Such pests may attack hosts that are widely dispersed throughout forests with high tree species diversity or may cause mortality or defoliation that is otherwise difficult to detect. A pathogen or insect might be considered a mortality-causing agent in one location and a defoliation-causing agent in another, depending on the level of damage to the forest in an area and the convergence of other stress factors such as drought. In some cases, the identified agents of mortality or defoliation are actually complexes of multiple agents summarized under an impact label related to a specific host tree species (e.g., “beech bark disease complex” or “yellow-cedar decline”). Additionally, differences in data collection, attribute recognition, and

coding procedures among States and regions can complicate data analysis and interpretation of the results. A recent comparison of aerial survey data with ground observations found that the accuracy of the aerial survey data exceeded 70 percent, that damage type observations for tree mortality and defoliation had high levels of accuracy, and that accuracy declined as the specificity for observations went from general to species level for tree species and damage agents, although many prominent tree species and agents had low to zero commission errors (Coleman and others 2018).

In 2019, IDS surveys of the CONUS covered about 219.00 million ha of both forested and unforested area (fig. 2.1), of which approximately 155.34 million ha encompassed tree canopy cover, or about 49.2 percent of the 315.99-million-ha tree canopy area of the CONUS. The entirety of this area was surveyed using the Digital Mobile Sketch Mapping (DMSM) approach, which recently replaced the legacy Digital Aerial Sketch Mapping (DASM) approach (Berryman and McMahan 2019). Meanwhile, roughly 10.8 percent (8.39 million ha) of Alaska's 77.78 million ha of forest or shrubland were surveyed in 2019, out of a total of 9.88 million ha surveyed across landcover types. In Hawaii, surveyors covered about 798 000 ha during 2019, of which approximately 551 000 ha had tree canopy cover, or about 63.9 percent of the 861 000 ha of total tree cover area in the State. Finally, 2019 surveys in the U.S. Caribbean territories of Puerto Rico and the U.S. Virgin Islands covered 99 percent of the 496 506 ha of tree canopy

cover area (491 523 ha). These Caribbean surveys did not record insect and disease damage, however, so these jurisdictions are not included in the analyses for this chapter.

Digital Mobile Sketch Mapping includes tablet hardware, software, and data support processes that allow trained aerial surveyors in light aircraft, as well as ground observers, to record forest disturbances and their causal agents. Digital Mobile Sketch Mapping enhances the quality and quantity of forest health data while having the potential to improve safety by integrating with programs such as operational remote sensing (ORS), which uses satellite imagery to monitor disturbances in areas of higher aviation risk (FHP 2019). Geospatial data collected with DMSM are stored in the national IDS database. In an important change from DASM, the new DMSM approach allows surveyors to both define the extent of an area experiencing damage and to estimate percent range of the area within the polygon that is affected. While additional validation will be required for this new metric, it is expected to increase the accuracy of derived damage metrics because it potentially corrects for previous overestimation caused by "lassoing" areas of undamaged trees into large areas of damage (ch. 12, Coleman and others 2018). For this reason, FHM reports before 2019 did not incorporate any derived damage estimates beyond the areal footprint damage with mortality or defoliation polygon boundaries, but these are now possible because of the inclusion of damage percentage estimates within polygons (see "Analyses" below).

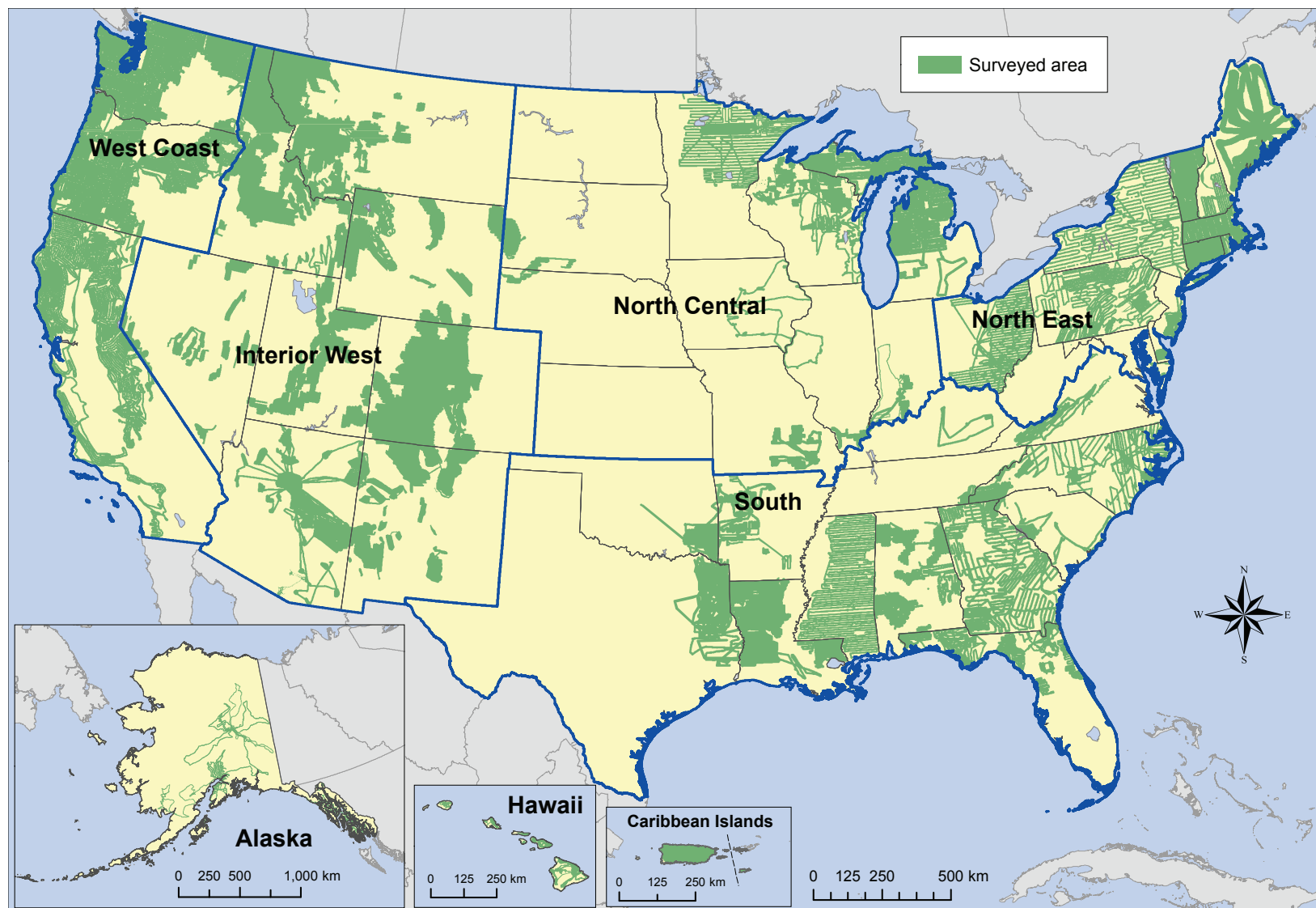


Figure 2.1—The extent of surveys for insect and disease activity conducted in the conterminous United States, Alaska, Hawaii, and the U.S. Caribbean Island territories in 2019. The blue lines delineate Forest Health Monitoring regions. Note: Alaska and Hawaii are not shown to scale with map of the conterminous United States. (Data source: U.S. Department of Agriculture Forest Service, Forest Health Protection)

Digital Mobile Sketch Mapping includes both polygon geometry, used for damage areas where boundaries are discrete and obvious from the air, and point geometry, used for small clusters of damage where the size and shape of the damage are less important than recording the location of damage, such as for sudden oak death (caused by the pathogen *Phytophthora ramorum*), southern pine beetle (*Dendroctonus frontalis*), and some types of bark beetle damage in the West. For the 2019 data, these points were assigned an area of 0.8 ha (about 2 acres). Additionally, DMSM allows for the use of grid cells (240-, 480-, 960-, or 1920-m resolution) to estimate the percentage of trees affected by damages that may be widespread and diffuse, such as those associated with European gypsy moth (*Lymantria dispar dispar*) and emerald ash borer. When calculating the total areas affected by each damage agent, we used the entire areas of these grid cells (e.g., 240-m cell = 5.76 ha).

Analyses

To estimate the extent of damaging insect and disease agents in 2019, we conducted two types of analyses. In the first, we reported the most widely detected mortality and defoliation agents in a series of tables. Specifically, the 2019 mortality and defoliation polygons were used to identify the select mortality and defoliation agents and complexes causing damage on >5000 ha of forest in the CONUS in that year. Similarly, we listed the five most widely reported mortality and defoliation agents and complexes within each of five FHM regions within the

CONUS (West Coast, Interior West, North Central, North East, and South), as well as for Alaska and Hawaii where data were available.

Because of the insect and disease aerial sketch-mapping process (i.e., digitization of polygons by a human interpreter aboard the aircraft), all quantities are approximate “footprint” areas for each agent or complex, delineating areas of visible damage within which the agent or complex is present. Unaffected trees may exist within the footprint, and the amount of damage within the footprint is not reflected in the estimates of forest area affected. The sum of areas affected by all agents and complexes is not equal to the total affected area as a result of overlapping polygons and the reporting of multiple agents per polygon in some situations.

In our second set of analyses, we used the IDS data for 2019 to more directly estimate the impacts of insect- and disease-related mortality and defoliation on U.S. forests. These results are reported in a set of figures describing (1) the percentage of surveyed tree canopy cover area with insect- and disease-related mortality or defoliation within ecoregions across the United States and (2) geographic hot spots of insect- and disease-related mortality or defoliation across the CONUS and within the five FHM regions.

As an indicator of the extent of damaging insect and disease agents, we summarized the percentage of surveyed tree canopy cover area experiencing mortality or defoliation for ecoregions within the CONUS and Hawaii, and

for surveyed forest and shrubland in Alaska ecoregions. This is a change from FHM reports before 2019, in which we reported on the percentage of regions *exposed to* mortality and defoliating agents based only on the footprint with mortality or defoliation polygon boundaries (masked by forest cover) because information on the percentage of damage within polygons was not yet completely available. As noted above, DMSM now allows surveyors both to define the extent of an area experiencing damage and to estimate percent range of the area within the polygon that is affected (specifically 1–3 percent, 4–10 percent, 11–29 percent, 30–50 percent, and >50 percent). By multiplying the area of damage within each polygon (after masking by tree canopy cover) by the midpoint of the estimated percent-affected range, it is possible to generate an adjusted estimate of the area affected by each mortality or defoliation agent detection (Berryman and McMahan 2019). These individual estimates can be summed for all the polygons within an ecoregion and divided by the total surveyed tree canopy cover area within the ecoregion to generate an estimate of the percentage of its canopy cover area affected by defoliating or mortality-causing agents. (Digital Mobile Sketch Mapping point data are also included in this estimate. Surveyors have the option to estimate the number of trees affected at a point and are required to assign an area value associated with each point, which is assumed to be 100 percent affected by its mortality or defoliation agent. For simplicity, we transformed each point into a 2-acre [0.809-ha] polygon. These areas for all

the points in an ecoregion were then added to the polygon-adjusted affected area estimates for the ecoregion.)

For the CONUS, percentage of surveyed tree canopy area with mortality or defoliation was calculated within each of 190 ecoregion sections (Cleland and others 2007). Similarly, the mortality and defoliation data were summarized for each of the 32 ecoregion sections in Alaska (Spencer and others 2002). In Hawaii, the percentage of surveyed tree canopy area affected by mortality and defoliation agents was calculated by ecoregions on each of the major islands of the archipelago (Potter 2020). Statistics were not calculated for analysis regions in the CONUS or Hawaii with <5 percent of the tree canopy cover area surveyed, nor in Alaska with <2.5 percent of the forest and shrubland area surveyed.

The tree canopy data used for the CONUS and Hawaii were resampled to 240 m from a 30-m raster dataset that estimates percentage of tree canopy cover (from 0 to 100 percent) for each grid cell; this dataset was generated from the 2011 National Land Cover Database (NLCD) (Homer and others 2015) through a cooperative project between the Multi-Resolution Land Characteristics Consortium and the Forest Service Geospatial Technology and Applications Center (GTAC) (Coulston and others 2012). For our purposes, we treated any cell with >0-percent tree canopy cover as forest. Comparable tree canopy cover data were not available for Alaska, so we instead created a 240-m-resolution layer of forest and shrub

cover from the 2011 NLCD. (This is different than Forest Health Monitoring national reports previous to 2019, for which the mortality and defoliation polygons were masked using a forest cover map [1-km resolution] derived from Moderate Resolution Imaging Spectroradiometer [MODIS] imagery by the Forest Service GTAC [USDA Forest Service 2008].)

Additionally, we used the Spatial Association of Scalable Hexagons (SASH) analytical approach to identify statistically significant geographic hot spots of mortality or defoliation in the CONUS. This method identifies locations where ecological phenomena occur at greater or lower frequency than expected by random chance and is based on a sampling frame optimized for spatial neighborhood analysis, adjustable to the appropriate spatial resolution, and applicable to multiple data types (Potter and others 2016). Specifically, it consists of dividing an analysis area into scalable equal-area hexagonal cells within which data are aggregated, followed by identifying statistically significant geographic clusters of hexagonal cells within which mean values are greater or less than those expected by chance. To identify these clusters, we employed a Getis-Ord (G_i^*) hot spot analysis (Getis and Ord 1992) in ArcMap® 10.3 (ESRI 2017). We conducted two sets of hot spot analyses for both mortality-causing and defoliation-causing agents: one for the CONUS in its entirety, and one for each of the five FHM regions within the CONUS. The low density of survey data in 2019 from Alaska and the small spatial extent of Hawaii (fig. 2.1) precluded

the use of Getis-Ord G_i^* hot spot analyses for these States.

The units of analysis were 9,810 hexagonal cells, each approximately 834 km² in area, generated in a lattice across the CONUS using intensification of the Environmental Monitoring and Assessment Program (EMAP) North American hexagon coordinates (White and others 1992). These coordinates are the foundation of a sampling frame in which a hexagonal lattice was projected onto the CONUS by centering a large base hexagon over the region (Reams and others 2005, White and others 1992). This base hexagon can be subdivided into many smaller hexagons, depending on sampling needs, and serves as the basis of the plot sampling frame for the Forest Inventory and Analysis (FIA) program (Reams and others 2005). Importantly, the hexagons maintain equal areas across the study region regardless of the degree of intensification of the EMAP hexagon coordinates. In addition, the hexagons are compact and uniform in their distance to the centroids of neighboring hexagons, meaning that a hexagonal lattice has a higher degree of isotropy (uniformity in all directions) than does a square grid (Shima and others 2010). These are convenient and highly useful attributes for spatial neighborhood analyses. These scalable hexagons also are independent of geopolitical and ecological boundaries, avoiding the possibility of different sample units (such as counties, States, or watersheds) encompassing vastly different areas (Potter and others 2016). We selected hexagons

834 km² in area because this is a manageable size for making monitoring and management decisions in analyses that are national in extent (Potter and others 2016).

The Getis-Ord G_i^* statistic was then used to identify clusters of hexagonal cells in which the percentage of surveyed tree canopy area with mortality or defoliation was higher than expected by chance. This statistic allows for the decomposition of a global measure of spatial association into its contributing factors, by location, and is therefore particularly suitable for detecting instances of nonstationarity in a dataset, such as when spatial clustering is concentrated in one subregion of the data (Anselin 1992). Hexagons were excluded if they contained <5-percent tree canopy cover or if <1 percent of the tree canopy cover was surveyed in 2019.

The Getis-Ord G_i^* statistic for each hexagon summed the differences between the mean values in a local sample, determined by a moving window consisting of the hexagon and its 18 first- and second-order neighbors (the 6 adjacent hexagons and the 12 additional hexagons contiguous to those 6) and a global mean. Our first analysis encompassed a global mean of all the forested hexagonal cells in the CONUS, while we conducted another set of analyses separately within each of the five FHM regions. The G_i^* statistic was standardized as a z-score with a mean of 0 and a standard deviation of 1, with values >1.96 representing significant ($p < 0.025$) local clustering of high values and values <-1.96 representing significant

clustering of low values ($p < 0.025$), since 95 percent of the observations under a normal distribution should be within approximately two (exactly 1.96) standard deviations of the mean (Laffan 2006). In other words, a G_i^* value of 1.96 indicates that the local mean of the percentage of forest exposed to mortality-causing or defoliation-causing agents for a hexagon and its 18 neighbors is approximately two standard deviations greater than the mean expected in the absence of spatial clustering, while a G_i^* value of -1.96 indicates that the local mortality or defoliation mean for a hexagon and its 18 neighbors is approximately two standard deviations less than the mean expected in the absence of spatial clustering. Values between -1.96 and 1.96 have no statistically significant concentration of high or low values. In other words, when a hexagon has a G_i^* value between -1.96 and 1.96, mortality or defoliation damage within it and its 18 neighbors is not statistically different from a normal expectation. As described in Laffan (2006), it is calculated as:

$$G_i^* (d) = \frac{\sum_j w_{ij}(d) x_j - W_i^* \bar{x}^*}{s^* \sqrt{\frac{(ns_{1i}^*) - W_i^{*2}}{n-1}}}$$

where

G_i^* = the local clustering statistic (in this case, for the target hexagon)

i = the center of local neighborhood (the target hexagon)

d = the width of local sample window (the target hexagon and its first- and second-order neighbors)

x_j = the value of neighbor j

w_{ij} = the weight of neighbor j from location i (all the neighboring hexagons in the moving window were given an equal weight of 1)

n = number of samples in the dataset (the 4,303 hexagons containing >5 percent tree cover and with at least 1 percent of the canopy cover surveyed)

W_i^* = the sum of the weights

s_{1i}^* = the number of samples within d of the central location (19: the focal hexagon and its 18 first- and second-order neighbors)

\bar{x}^* = mean of whole dataset (in this case, the 4,303 hexagons)

s^* = the standard deviation of whole dataset (for the 4,303 hexagons)

It is worth noting that the -1.96 and 1.96 threshold values are not exact because the correlation of spatial data violates the assumption of independence required for statistical significance (Laffan 2006). The Getis-Ord approach does not require that the input data be normally distributed because the local G_i^* values are computed under a randomization assumption, with G_i^* equating to a standardized z-score that asymptotically tends to a normal distribution (Anselin 1992). The z-scores are reliable, even with skewed data, as long as the distance band used to define the local sample

around the target observation is large enough to include several neighbors for each feature (ESRI 2017).

RESULTS AND DISCUSSION

Conterminous United States Mortality

The national IDS data in 2019 identified 58 mortality-causing agents and complexes across the CONUS on an area slightly larger than the combined land area of Vermont and Rhode Island (approximately 2.69 million ha). In comparison, forests cover approximately 252 million ha of the CONUS (Smith and others 2009). Twenty-one of the agents were detected on >5000 ha.

As in 2018 (Potter and others 2020b), fir engraver (*Scolytus ventralis*) was the most widespread mortality agent in 2019, detected on approximately 1.09 million ha (table 2.1), or about 40.5 percent of the total mortality area, followed by emerald ash borer, which was identified on about 517 000 ha. Three additional mortality agents and complexes were detected on >100 000 ha: pinyon ips (*Ips confusus*) on 126 000 ha, mountain pine beetle (*D. ponderosae*) on 122 000 ha, and unknown bark beetles on 116 000 ha (mostly damage on ponderosa pines [*Pinus ponderosa*] in the Interior West by a list of various bark beetle species that are not possible to distinguish from the air). Mortality from the western bark beetle group, including 16 different agents in the IDS data (table 2.2), encompassed about 64 percent of all the 2019 mortality area across the CONUS.

Table 2.1—Mortality agents and complexes affecting >5000 ha in the conterminous United States during 2019

Agents/complexes causing mortality, 2019	Area <i>ha</i>
Fir engraver	1 088 757
Emerald ash borer	517 163
Pinyon ips	125 813
Mountain pine beetle	121 932
Unknown bark beetle ^a	116 053
Eastern larch beetle	99 768
Gypsy moth	97 973
Western pine beetle	90 015
Spruce beetle	77 435
Douglas-fir beetle	71 971
Balsam woolly adelgid	69 357
Unknown	42 404
Sudden oak death	37 043
Flatheaded fir borer	34 716
Jeffrey pine beetle	27 155
Subalpine fir decline	24 035
Western balsam bark beetle	23 047
Cedar and cypress bark beetles	18 049
Beech bark disease complex	8959
Roundheaded pine beetle	8790
Ips engraver beetles	7428
Other (37)	28 653
Total, all mortality agents	2 685 933

Note: All values are “footprint” areas for each agent or complex. The sum of the individual agents is not equal to the total for all agents due to the reporting of multiple agents per polygon.

^a In the Interior West, this is primarily damage on ponderosa pines. The group of bark beetles is known and varied but not distinguishable from the air. Regions have characterized it as “Southwest bark beetle complex” consisting mainly of damage caused by roundheaded pine beetle, western pine beetle, and ips beetles.

Table 2.2—Beetle taxa included in the “western bark beetle” group

Western bark beetle mortality agents	
Cedar and cypress bark beetles	<i>Phloeosinus</i> spp.
Douglas-fir beetle	<i>Dendroctonus pseudotsugae</i>
Douglas-fir engraver	<i>Scolytus unispinosus</i>
Fir engraver	<i>Scolytus ventralis</i>
Ips engraver beetles	<i>Ips</i> spp.
Jeffrey pine beetle	<i>Dendroctonus jeffreyi</i>
Mountain pine beetle	<i>Dendroctonus ponderosae</i>
Pine engraver	<i>Ips pini</i>
Pinyon ips	<i>Ips confusus</i>
Root disease and beetle complex	--
Roundheaded pine beetle	<i>Dendroctonus adjunctus</i>
Silver fir beetle	<i>Pseudohylesinus sericeus</i>
Spruce beetle	<i>Dendroctonus rufipennis</i>
Unknown bark beetle	--
Western balsam bark beetle	<i>Dryocoetes confusus</i>
Western pine beetle	<i>Dendroctonus brevicomis</i>

Also, as in the previous year, the FHM West Coast region in 2019 had the largest area on which mortality agents and complexes were detected, about 1.36 million ha (table 2.3). Three-quarters of this area (1 028 000 ha) was associated with fir engraver mortality. The next most commonly detected mortality agents were western pine beetle (*D. brevicomis*) on 89 000 ha (6.6 percent of the mortality area), mountain pine beetle on 76 000 ha (5.6 percent), sudden oak death on 37 000 ha (2.7 percent), and Douglas-fir beetle (*D. pseudotsugae*) on 36 000 ha

Table 2.3—The top five mortality agents or complexes for each Forest Health Monitoring region, and for Alaska and Hawaii, in 2019

Mortality agents and complexes, 2019	Area	Mortality agents and complexes, 2019	Area	Mortality agents and complexes, 2019	Area
	ha		ha		ha
Interior West		South		Hawaii	
Pinyon ips	125 798	Unknown	3795	Unknown ^b	27 237
Unknown bark beetle ^a	114 206	Emerald ash borer	2430	Total, all mortality agents and complexes	27 237
Spruce beetle	76 782	Ips engraver beetles	1468	<p>Note: The total area affected by other agents is listed at the end of each section. All values are “footprint” areas for each agent or complex. The sum of the individual agents is not equal to the total for all agents due to the reporting of multiple agents per polygon.</p> <p>^a In the Interior West, this is primarily damage on ponderosa pines. The group of bark beetles is known and varied but not distinguishable from the air. Regions have characterized it as “Southwest bark beetle complex” consisting mainly of damage caused by roundheaded pine beetle, western pine beetle, and ips beetles.</p> <p>^b Most of the mortality recorded in Hawaii is coded as “unknown” mortality on ‘ōhi‘a lehua. Damage is likely attributed to rapid ‘ōhi‘a death but has not been confirmed.</p>	
Balsam woolly adelgid	62 517	Southern pine beetle	286		
Fir engraver	60 831	Black turpentine beetle	<1		
Other mortality agents (16)	151 449	Other mortality agents (1)	<1		
Total, all mortality agents and complexes	565 807	Total, all mortality agents and complexes	7979		
North Central		West Coast			
Emerald ash borer	416 876	Fir engraver	1 027 926		
Eastern larch beetle	99 768	Western pine beetle	89 410		
Beech bark disease complex	8665	Mountain pine beetle	75 690		
Unknown	5338	Sudden oak death	37 043		
Unknown bark beetle	1278	Douglas-fir beetle	35 914		
Other mortality agents (12)	2683	Other mortality agents (18)	122 311		
Total, all mortality agents and complexes	534 585	Total, all mortality agents and complexes	1 363 297		
North East		Alaska			
Gypsy moth	97 973	Spruce beetle	53 900		
Emerald ash borer	97 856	Yellow-cedar decline	8088		
Linden looper	4153	Northern spruce engraver	433		
Southern pine beetle	3033	Western balsam bark beetle	43		
Black turpentine beetle	2822	Unknown canker	29		
Other mortality agents (21)	8438	Other mortality agents (1)	4		
Total, all mortality agents and complexes	214 265	Total, all mortality agents and complexes	62 497		

(2.6 percent). Another 18 mortality-causing agents and complexes accounted for 8.9 percent of the mortality area in the West Coast region.

A handful of ecoregion sections in the West Coast region had relatively high percentages of mortality of surveyed tree canopy area, especially the M261E–Sierra Nevada ecoregion section in California (1.47 percent) and the M261A–Klamath Mountains ecoregion section in northwestern California and southwestern Oregon (1.01 percent) (fig. 2.2). The mortality in these regions was primarily caused by infestation of fir engraver in red fir (*Abies magnifica*) and white fir (*A. concolor*) and resulted in a series of geographic hot spots of high mortality in analyses conducted both for the CONUS (fig. 2.3A) and limited to the West Coast FHM region (fig. 2.3B). Fir engraver also impacted neighboring ecoregion sections, including M261D–Southern Cascades (0.68-percent mortality of surveyed canopy area), M261G–Modoc Plateau (0.65 percent), and M261B–Northern California Coast Ranges (0.58 percent). Flatheaded fir borer (*Phaenops drummondi*) in Douglas-fir (*Pseudotsuga menziesii*) was also an issue in the northern (Oregon) portions of M261A–Klamath Mountains.

Fir engraver, along with western pine beetle in ponderosa pine stands, resulted in moderately high mortality (0.70 percent of the surveyed tree canopy cover) in the M332G–Blue Mountains ecoregion section of northeastern Oregon (fig. 2.2), as well as a moderate-mortality hot spot (fig. 2.3). Along with fir engraver, western pine beetle and mountain pine beetle were

issues in nearby M242D–Northern Cascades (0.48 percent), M242C–Eastern Cascades (0.35 percent), M333A–Okanogan Highland (0.35 percent), and 342H–Blue Mountain Foothills (0.28 percent).

Elsewhere in the West Coast region, sudden oak death in tanoak (*Notholithocarpus densiflorus*) resulted in 0.48-percent mortality of surveyed canopy area in 263A–Northern California Coast and 0.31 percent in 261A–Central California Coast.

In 2019, the FHM Interior West region had the second most extensive area of insect and disease mortality detection, with 21 agents and complexes identified across 566 000 ha (table 2.3). Unlike in 2018, when spruce beetle (*D. rufipennis*) was the most widely detected agent, pinyon ips damage was recorded on the most area, about 126 000 ha, or 22.2 percent of the total mortality area. Meanwhile, unknown bark beetles affected 20.2 percent of the total mortality area, or 114 000 ha. This was primarily damage on ponderosa pines by a group of known and varied bark beetles that are not distinguishable from the air. This has been characterized as “Southwest bark beetle complex” consisting mainly of damage caused by roundheaded pine beetle (*D. adjunctus*), western pine beetle, and ips beetles. Other widespread mortality agents were spruce beetle detected on 77 000 ha (13.6 percent), balsam woolly adelgid (*Adelges piceae*) on 63 000 ha (11.0 percent), and fir engraver beetle on 61 000 ha (10.8 percent) (table 2.3).

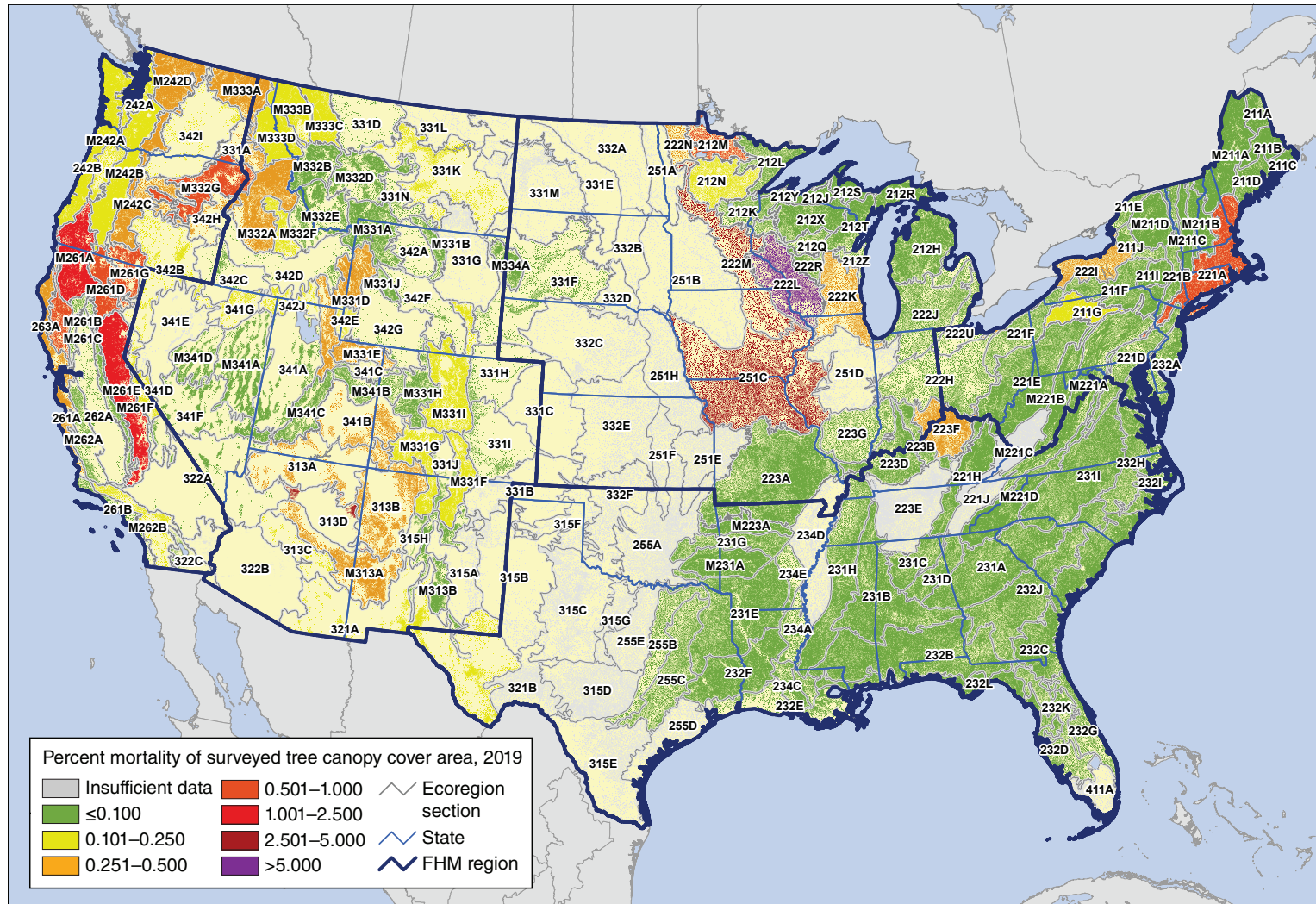


Figure 2.2—The percentage of surveyed tree canopy cover area with insect and disease mortality, by ecoregion section within the conterminous 48 States, for 2019. The gray lines delineate ecoregion sections (Cleland and others 2007). The 240-m tree canopy cover is based on data from a cooperative project between the Multi-Resolution Land Characteristics Consortium (Coulston and others 2012) and the Forest Service Geospatial Technology and Applications Center using the 2011 National Land Cover Database. (Data source: U.S. Department of Agriculture Forest Service, Forest Health Protection)

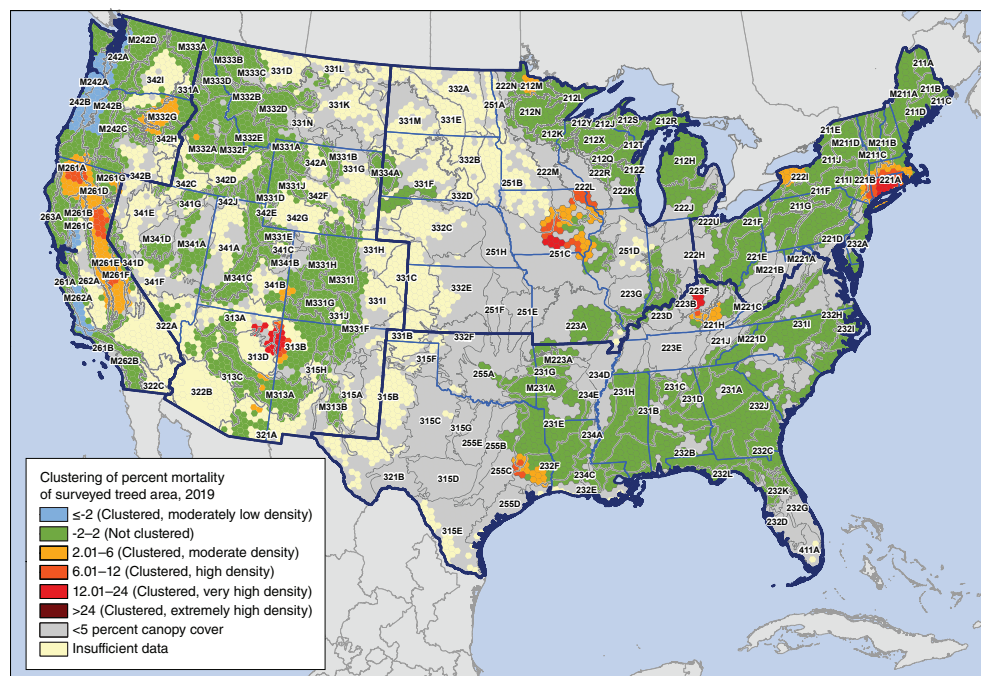
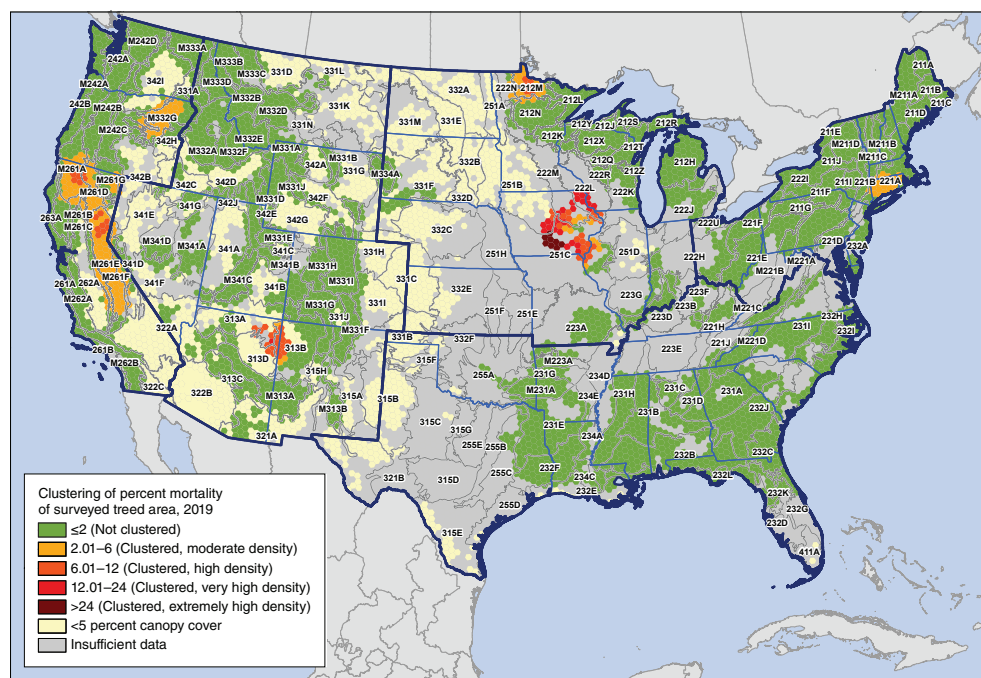


Figure 2.3—Hot spots of percentage of surveyed tree canopy cover area with insect and disease mortality in 2019 for (A) the conterminous 48 States and (B) for separate Forest Health Monitoring (FHM) regions, by hexagons containing > 5 -percent tree canopy cover. Values are Getis-Ord G_i^* scores, with values > 2 representing significant clustering of high mortality occurrence densities and values < -2 representing significant clustering of low mortality occurrence densities. The gray lines delineate ecoregion sections (Cleland and others 2007), and blue lines delineate FHM regions. Tree canopy cover is based on data from a cooperative project between the Multi-Resolution Land Characteristics Consortium (Coulston and others 2012) and the Forest Service Geospatial Technology and Applications Center using the 2011 National Land Cover Database. (Data source: U.S. Department of Agriculture Forest Service, Forest Health Protection)

Interior West mortality was highest in northeastern Arizona and northwestern New Mexico, where two nearly adjacent hot spots were detected of mostly high mortality density in the CONUS hot spot analysis and of very high density in the regional analysis (fig. 2.3). The primary causes of mortality in this area were the “Southwest bark beetle complex” in ponderosa pine stands, described above, and pinyon ips in two-needle pinyon (*P. edulis*) stands. As a result of these agents, the 313D–Painted Desert ecoregion section had the highest percentage of surveyed tree canopy area mortality (4.69) in the Interior West region (fig. 2.2). Adjacent ecoregion sections also had relatively high mortality percentages: 313B–Navajo Canyonlands (0.35), M313A–White Mountains–San Francisco Peaks–Mogollon Rim (0.28), and 313A–Grand Canyon (0.27).

These agents, as well as roundheaded pine beetle (*D. adjunctus*) in ponderosa pine, spruce beetle in Engelmann spruce (*Picea engelmannii*), subalpine fir (*A. lasiocarpa*) decline, and Douglas-fir beetle, resulted in relatively high mortality (0.38 percent of surveyed canopy area) in the 341B–Northern Canyonlands ecoregion section of southwestern Colorado and southeastern Utah (fig. 2.2). The regional hot spot analysis detected an area of moderate mortality density in this area as well (fig. 2.3B). Further north, in northeastern Utah, southeastern Idaho, and western Wyoming, balsam woolly adelgid and subalpine fir decline in subalpine fir stands, as well as spruce beetle in Engelmann spruce stands, caused moderate levels of mortality in M331E–Uinta Mountains (0.34 percent) and

M331D–Overthrust Mountains (0.28 percent). Finally, two ecoregion sections in central Idaho (M332A–Idaho Batholith and 331A–Palouse Prairie) both had 0.39-percent mortality in surveyed treed area because of mountain pine beetle in lodgepole pine (*P. contorta*), balsam woolly adelgid and subalpine fir decline in subalpine fir, fir engraver in grand fir (*A. grandis*), and Douglas-fir beetle. A small hot spot of moderate mortality was detected in this area in the regional analysis (fig. 2.3B).

In the FHM North Central region, meanwhile, surveyors recorded approximately 535 000 ha with mortality in 2019.

Of this footprint, about 78 percent was attributed to emerald ash borer (417 000 ha) and 19 percent to eastern larch beetle (*D. simplex*, 100 000 ha) (table 2.3). Of the other 15 mortality agents recorded, beech bark disease complex was the most widespread (1.6 percent of the mortality area).

The ecoregion section with the greatest mortality of surveyed tree canopy cover nationally was 222L–North Central U.S. Driftless and Escarpment of southwestern Wisconsin, northeastern Iowa, and southeastern Minnesota (6.7 percent), where emerald ash borer was detected killing white, green, and black ash (*Fraxinus americana*, *F. pennsylvanica*, and *F. nigra*) (fig. 2.2). Two adjacent ecoregion sections also experienced extensive mortality associated with emerald ash borer: 251C–Central Dissected Till Plains of southeastern Iowa (5.0 percent) and 222M–Minnesota and Northeast Iowa

Morainal-Oak Savannah (2.63 percent). This mortality resulted in a hot spot of extremely high mortality density in the CONUS analysis (fig. 2.3A) and of very high mortality density in the regional analysis (fig. 2.3B).

A second hot spot of mortality, of high mortality density in the national analysis and moderate mortality density in the regional analysis, was detected in 212M–Northern Minnesota and Ontario, where an ongoing eastern larch beetle infestation is affecting tamarack (*Larix laricina*). In this ecoregion section, 0.94 percent of surveyed tree canopy cover experienced mortality (fig. 2.2).

In the North East FHM region, 26 mortality agents and complexes were recorded in 2019 on a total of approximately 214 000 ha (table 2.3). The most common were gypsy moth and emerald ash borer, both identified on about 98 000 ha (45.7 percent of the total mortality area in the region). Other less common agents were linden looper (*Erannis tiliaria*, 1.9 percent), southern pine beetle (1.4 percent), and black turpentine beetle (*Dryocoetes confusus*, 1.3 percent).

The 221A–Lower New England ecoregion section experienced 0.77-percent mortality within the surveyed tree canopy cover area, resulting from widespread gypsy moth impacts in deciduous forests in addition to some emerald ash borer-caused mortality in ash stands of Massachusetts, Connecticut, and Rhode Island. This ecoregion also had southern pine beetle and oak wilt mortality on

Long Island (fig. 2.2). The mortality in this area resulted in a hot spot of very high mortality density in the regional analysis, and one of moderate mortality density in the CONUS analysis (fig. 2.3).

Two other ecoregion sections, 222I–Erie and Ontario Lake Plain in western New York (0.33 percent) and 211G–Northern Unglaciaded Allegheny Plateau in north-central Pennsylvania (0.12 percent) were also the locations of relatively high mortality associated with emerald ash borer. The former of these caused a moderate mortality hot spot in the regional analysis.

Finally, in the South FHM region, surveyors identified six agents resulting in 8000 ha with mortality (table 2.3). The most common mortality category was “unknown” (3800 ha, 47.6 percent) followed by emerald ash borer (2400 ha, 30.5 percent) and ips engraver beetles (1500 ha, 18.4 percent). Southern pine beetle was found on an additional 286 ha (3.6 percent).

A single ecoregion section in the South had mortality exceeding 0.1 percent of the surveyed tree canopy area. This was 223F–Interior Low Plateau-Bluegrass (0.45 percent) in northern Kentucky where emerald ash borer was relatively widely detected (fig. 2.2). Regional hot spots of mortality were detected here and in three ecoregion sections of eastern Texas (232F–Coastal Plains and Flatwoods-Western Gulf, 255C–Oak Woods and Prairie,

and 231E–Mid Coastal Plains–Western) where there was ips engraver beetle activity in yellow pine forests and hardwood mortality with an unknown cause (fig. 2.3B).

Conterminous United States Defoliation

The national IDS in 2019 identified 64 defoliation agents and complexes affecting approximately 1.42 million ha across the CONUS (table 2.4), which is somewhat smaller than the combined land area of Connecticut and Rhode Island. As in 2018 (Potter and others 2020b), the most widespread defoliation agent was western spruce budworm (*Choristoneura freemani*), detected on approximately 41 percent of the total area with defoliation (589 000 ha). Four additional agents were each detected on >100 000 ha: hemlock looper (*Lambdina fiscellaria*) on 170 000 ha, forest tent caterpillar (*Malacosoma disstria*) on 116 000 ha, spruce budworm (*C. fumiferana*) on 112 000 ha, and Douglas-fir tussock moth (*Orgyia pseudotsugata*) on 100 000 ha (table 2.4).

The FHM region with by far the largest area on which defoliation agents were detected in 2019 was the Interior West, with 957 000 ha of damage associated with 24 defoliators (table 2.5). As in 2018, the majority of this area (61.5 percent) was affected by western spruce budworm (588 000 ha). Hemlock looper affected 168 000 ha (17.6 percent of the total), Douglas-fir tussock moth 92 000 ha (9.6 percent), Marssonina blight (*Drepanopeziza* spp.) 36 000 ha (3.8 percent), and pinyon needle scale (*Matsucoccus acalyptus*) 26 000 ha (2.7 percent).

Table 2.4—Defoliation agents and complexes affecting >5000 ha in the conterminous United States in 2019

Agents/complexes causing defoliation, 2019	Area
	ha
Western spruce budworm	588 591
Hemlock looper	170 011
Forest tent caterpillar	116 395
Spruce budworm	111 754
Douglas-fir tussock moth	100 142
Gypsy moth	93 155
Marssonina blight	37 966
Baldcypress leafroller	35 302
Gelechiid moths/needleminers	30 313
Pinyon needle scale	27 979
Unknown defoliator	25 410
Balsam woolly adelgid	16 212
Jumping oak gall wasp	12 389
Spruce aphid	11 173
White pine needle damage	9419
Maple leafcutter	6543
Aspen blotchminer	6232
Unknown	6087
Yellow poplar weevil	5444
Other (45)	41 456
Total, all defoliation agents	1 419 839

Note: All values are “footprint” areas for each agent or complex. The sum of the individual agents is not equal to the total for all agents due to the reporting of multiple agents per polygon.

Table 2.5—The top five defoliation agents or complexes for each Forest Health Monitoring region and for Alaska and Hawaii, in 2019

Defoliation agents and complexes, 2019	Area	Defoliation agents and complexes, 2019	Area	Defoliation agents and complexes, 2019	Area
	ha		ha		ha
Interior West		South		Hawaii	
Western spruce budworm	587 931	Forest tent caterpillar	65 541	‘Ōhi’a/guava rust	5
Hemlock looper	167 884	Baldcypress leafroller	35 302	Total, all mortality agents and complexes	5
Douglas-fir tussock moth	92 155	Yellow poplar weevil	5403	Note: The total area affected by other agents is listed at the end of each section. All values are “footprint” areas for each agent or complex. The sum of the individual agents is not equal to the total for all agents due to the reporting of multiple agents per polygon.	
Marssonina blight	36 313	Walkingstick	4567		
Pinyon needle scale	26 123	Gypsy moth	3571	^a There was no Swiss needle cast survey in 2019.	
Other defoliation agents (19)	56 904	Other defoliation agents (4)	3520		
Total, all defoliation agents and complexes	956 527	Total, all defoliation agents and complexes	96 742		
North Central		West Coast^a			
Spruce budworm	111 754	Balsam woolly adelgid	16 212		
Gypsy moth	79 235	Gelechiid moths/needleminers	8018		
Forest tent caterpillar	48 972	Douglas-fir tussock moth	7987		
Jumping oak gall wasp	12 389	Spruce aphid	7890		
Aspen blotchminer	6232	Lodgepole needleminer	4764		
Other defoliation agents (10)	4665	Other defoliation agents (19)	17 758		
Total, all defoliation agents and complexes	263 243	Total, all defoliation agents and complexes	62 610		
North East		Alaska			
Gypsy moth	10 348	Hemlock sawfly	154 050		
White pine needle damage	9419	Birch leafminer	113 382		
Maple leafcutter	6543	Aspen leafminer	53 452		
Browntail moth	4993	Willow leaf blotchminer	12 853		
Unknown	2493	Unknown defoliator	5284		
Other defoliation agents (16)	7087	Other defoliation agents (4)	599		
Total, all defoliation agents and complexes	40 718	Total, all defoliation agents and complexes	339 601		

As in 2018, several ecoregion sections of the northern Rockies were severely affected by western spruce budworm in 2019, particularly two in southwestern Montana and east-central Idaho: M332E–Beaverhead Mountains and M332B–Northern Rockies and Bitterroot Valley with 3.94 percent and 2.93 percent of surveyed tree canopy area defoliated, respectively (fig. 2.4). The western spruce budworm defoliation extended into several ecoregion sections to the east, north, and south of these: M332D–Belt Mountains (2.18 percent), M331D–Overthrust Mountains (1.57 percent), M332F–Challis Volcanics (1.95 percent), M331A–Yellowstone Highlands (1.19 percent), M331B–Bighorn Mountains (1.15 percent), and M333C–Northern Rockies: (0.51 percent). To the west, M332A–Idaho Batholith (3.51-percent defoliation) experienced infestations of hemlock looper, Douglas-fir tussock moth, and western spruce budworm, while M333D–Bitterroot Mountains (2.76 percent) had extensive defoliation by hemlock looper. The northern Rockies area was encompassed by several adjacent hot spots of moderate to very high defoliation density in the analyses both for the entire CONUS (fig. 2.5A) and for the Interior West region (fig. 2.5B).

Farther south, an area of relatively high defoliation was centered on two ecoregion sections in south-central Colorado and northern New Mexico, M331F–Southern Parks and Rocky Mountain Range (3.31-percent defoliation) and M331G–South-Central Highlands (2.72 percent). Western spruce budworm was again the leading

defoliating agent, along with Marssonina blight in quaking aspen (*Populus tremuloides*) stands and Gelechiid moths/needleminers (*Coleotechnites* spp.) in ponderosa pine stands. The work of these agents resulted in a hot spot of high defoliation density in the CONUS analysis (fig. 2.5A) and a couple of hot spots of moderate defoliation density in the regional analysis (fig. 2.5B).

In south-central Utah, a hot spot of moderate defoliation was the result of a western spruce budworm infestation in M341C–Utah High Plateau (0.99-percent defoliation of surveyed canopy area).

The North Central FHM region, meanwhile, had 263 000 ha with defoliation associated with 15 agents and complexes, with spruce budworm the most widely detected (112 000 ha, 42.5 percent of the total) (table 2.5). Gypsy moth also caused widespread damage (79 000 ha, 30.1 percent), as did forest tent caterpillar (49 000 ha, 18.6 percent). Jumping oak gallwasp (*Neuroterus saltatorius*) and aspen blotchminer (*Phyllonorycter tremuloidiella*) were also somewhat widespread (4.7 percent and 2.4 percent of the regional total defoliation, respectively).

Defoliation in the North Central region was most widespread in the Great Lakes States (fig. 2.4), especially 212R–Eastern Upper Peninsula (2.00 percent of surveyed area with canopy cover), where forest tent caterpillar was the most commonly detected agent along with spruce budworm and jack pine budworm (*C. pinus*). In 212H–Northern Lower Peninsula

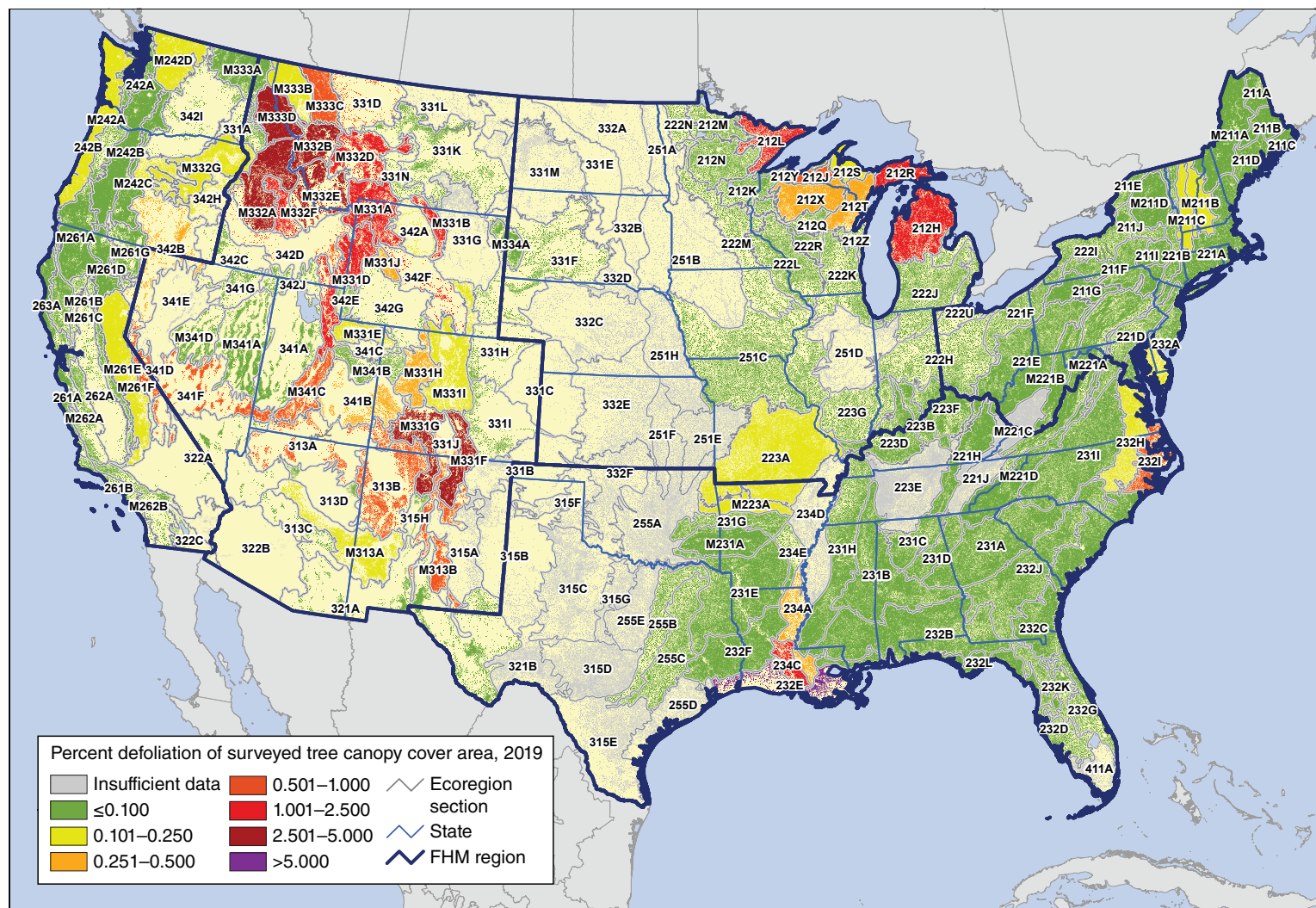


Figure 2.4—The percentage of surveyed tree canopy cover area with insect and disease defoliation, by ecoregion section within the conterminous 48 States, for 2019. The gray lines delineate ecoregion sections (Cleland and others 2007). The 240-m tree canopy cover is based on data from a cooperative project between the Multi-Resolution Land Characteristics Consortium (Coulston and others 2012) and the Forest Service Geospatial Technology and Applications Center using the 2011 National Land Cover Database. (Data source: U.S. Department of Agriculture Forest Service, Forest Health Protection)

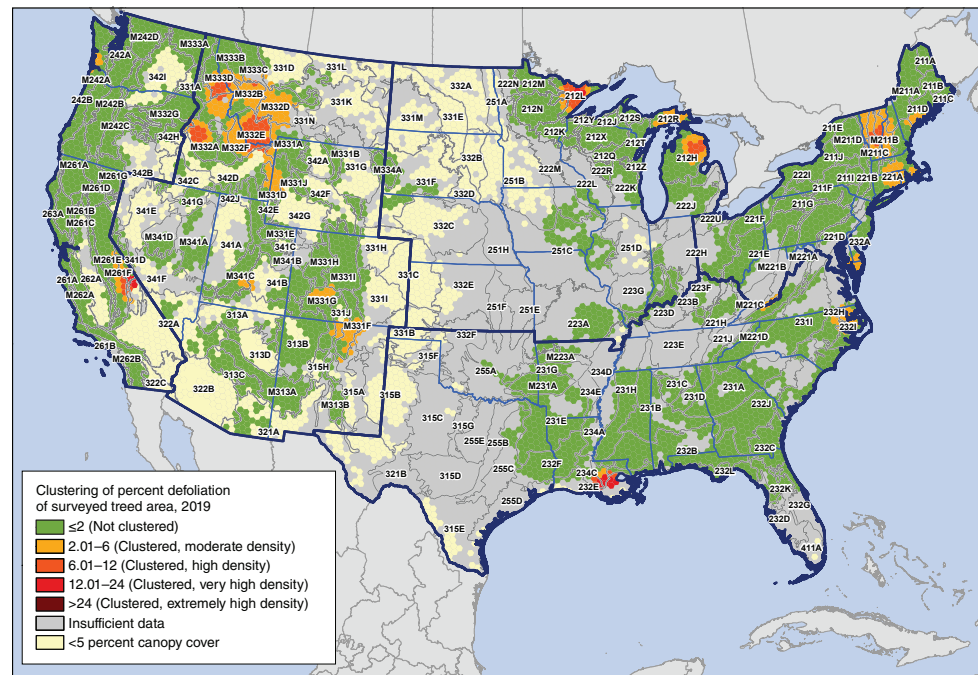
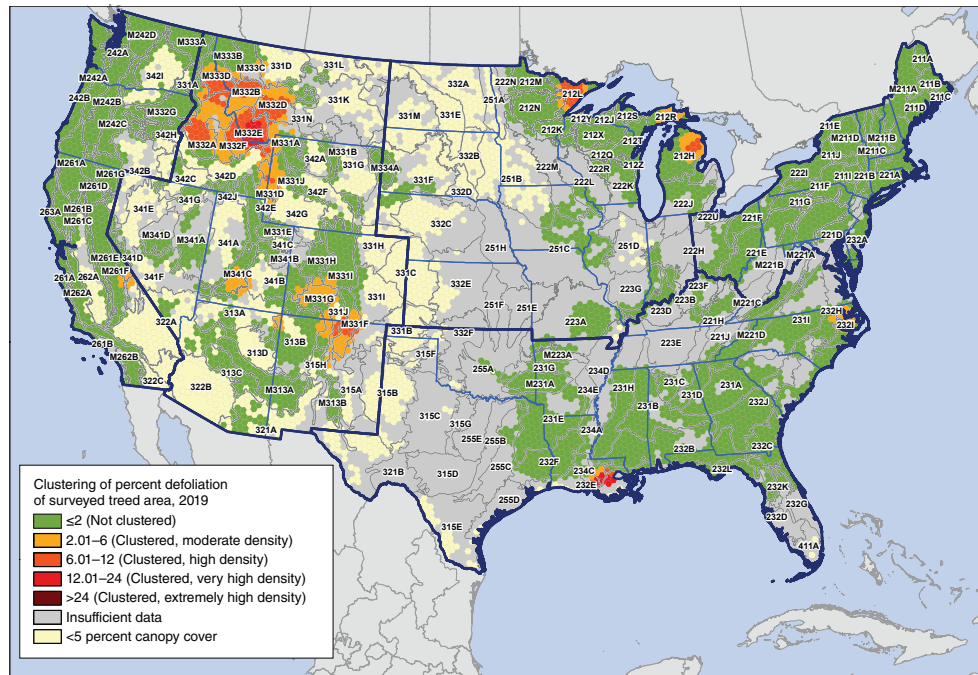


Figure 2.5—Hot spots of percentage of surveyed tree canopy cover area with insect and disease defoliation in 2019 for (A) the conterminous 48 States and (B) for separate Forest Health Monitoring regions, by hexagons containing >5 percent tree canopy cover. Values are Getis-Ord G_i^* scores, with values >2 representing significant clustering of high defoliation occurrence densities. (No areas of significant clustering of low densities, <-2, were detected.) The gray lines delineate ecoregion sections (Cleland and others 2007), and blue lines delineate Forest Health Monitoring regions. Tree canopy cover is based on data from a cooperative project between the Multi-Resolution Land Characteristics Consortium (Coulston and others 2012) and the Forest Service Geospatial Technology and Applications Center using the 2011 National Land Cover Database. (Data source: U.S. Department of Agriculture Forest Service, Forest Health Protection)

(1.75 percent), gypsy moth in oak (*Quercus* spp.) stands was the main agent, in addition to spruce budworm and forest tent caterpillar. Finally, in 212L–Northern Superior Uplands (1.72 percent), spruce budworm was an issue in balsam fir (*A. balsamea*) and white and black spruce (*P. glauca* and *P. mariana*) stands and larch casebearer (*Coleophora laricella*) and forest tent caterpillar were additional but less significant problems. Each of these ecoregion sections was the location of a hot spot of either high or moderate defoliation density in both the CONUS and regional analyses (fig. 2.5). Four other ecoregion sections in the Great Lakes States also had relatively high defoliation as a result of spruce budworm and forest tent caterpillar:

- 212J–Southern Superior Uplands (0.52 percent)
- 212X–Northern Highlands (0.38 percent)
- 212T–Northern Green Bay Lobe (0.30 percent)
- 212S–Northern Upper Peninsula (0.15 percent)

At the southern edge of the North Central region, in 223A–Ozark Highlands in southern Missouri, jumping oak gall wasp was an issue, resulting in 0.16-percent defoliation of surveyed canopy cover.

Surveyors in 2019 documented about 97 000 ha with defoliation in the South (table 2.5), with forest tent caterpillar detected on about 66 000 ha, or 67.7 percent of the

area with defoliation, and baldcypress leafroller (*Archips goyerana*) detected on about 35 000 ha, or 36.5 percent of the area with defoliation. Of the seven other defoliating agents detected in 2019, yellow poplar weevil (*Odontopus calceatus*), walkingstick (*Diapheromera femorata*), and gypsy moth were recorded on an additional 5400 ha, 4600 ha, and 3600 ha, respectively.

As in 2018, the southern ecoregion sections with the highest percentage of defoliation were in southern Louisiana, as the result mainly of baldcypress leafroller: 232E–Louisiana Coastal Prairie and Marshes (7.33 percent) and 234C–Atchafalaya and Red River Alluvial Plains (1.42 percent) (fig. 2.4). Forest tent caterpillar was an issue in the neighboring 234A–Southern Mississippi Alluvial Plain (0.45 percent). These defoliators resulted in the area being the location of a hot spot of very high defoliation density (fig. 2.5).

Elsewhere in the South, forest tent caterpillar and, to a lesser degree loblolly pine sawfly (*N. taeda linearis*), caused relatively high levels of defoliation and a hot spot of moderate defoliation in two ecoregion sections of eastern North Carolina: 232I–Northern Atlantic Coastal Flatwoods (0.86-percent defoliation of surveyed canopy cover) and 232H–Middle Atlantic Coastal Plains and Flatwoods (0.20 percent). Additionally, an ongoing infestation of walkingstick in M223A–Boston Mountains of northern Arkansas resulted in 0.12-percent defoliation of surveyed tree canopy area there (fig. 2.4).

In 2019, 24 defoliating agents were recorded in the West Coast FHM region on 63 000 ha (table 2.5). (Unlike 2018, there was no Swiss needle cast survey.) No single agent was responsible for a majority of the defoliation, but balsam woolly adelgid was detected on 16 000 ha (25.9 percent of the regional total), while three agents were found on about 8000 ha: Gelechiid moths/needleminers, Douglas-fir tussock moth, and spruce aphid (*Elatobium abietinum*).

A variety of pests, including Gelechiid moths/needleminers in ponderosa pine forests, Marssonina blight in quaking aspen stands, and pinyon needle scale in singleleaf pinyon (*P. monophylla*) forests, resulted in moderately high levels of defoliation in two ecoregion sections of eastern California, extending into western Nevada and the Interior West FHM region: 341D–Mono and 341F–Southeastern Great Basin (both with 0.73-percent defoliation of surveyed canopy cover area) (fig. 2.4). This defoliation also caused the West Coast region’s only national defoliation hot spot (fig. 2.5A) as well as a hot spot of very high defoliation density in the regional analysis (fig. 2.5B). Another regional hot spot, this one of moderate defoliation, was detected on the Pacific Coast border between Washington and Oregon (M242A–Oregon and Washington Coast Ranges), where there was an outbreak of spruce aphid in Sitka spruce (*P. sitchensis*).

In the North East region, two of 21 agents were the most widely identified: gypsy moth on about 10 000 ha (25.4 percent of the regional

total) and white pine needle damage on about 9000 ha (23.1 percent). Maple leafcutter (*Paraclemensia acerifoliella*) and browntail moth (*Euproctis chrysorrhoea*) were also relatively widely detected, constituting 16.1 percent and 12.3 percent of the total defoliation, respectively (table 2.5).

White pine needle damage in stands of eastern white pine (*P. strobus*) and maple leafcutter infestation in sugar maple (*Acer saccharum*) forests resulted in moderately high defoliation in the upper New England ecoregion sections of M211C–Green-Taconic-Berkshire Mountains (0.21 percent) and M211B–New England Piedmont (0.22 percent). These caused a regional geographic hot spot of high defoliation in the area (fig. 2.5B). Other North East region hot spots were associated with browntail moth in northern red oak (*Q. rubra*) stands in 211D–Central Maine Coastal and Embayment; with fall cankerworm (*Alsophila pometaria*) in eastern Massachusetts and gypsy moth in Connecticut and central Massachusetts (both in 221A–Lower New England); and with forest tent caterpillar and gypsy moth in the Delmarva Peninsula (232H–Middle Atlantic Coastal Plains and Flatwoods).

Alaska and Hawaii

In Alaska, six mortality agents and complexes were detected on approximately 62 000 ha in 2019 (table 2.3), a decline from the previous year. Spruce beetle was again the most widely detected mortality agent, representing 86.2 percent of the total area with mortality (54 000 ha). Most of the rest of the State’s

mortality was associated with yellow-cedar (*Chamaecyparis nootkatensis*) decline (8000 ha, 12.9 percent of the total).

As in 2018, the spruce beetle outbreak was focused in the south-central part of the State (fig. 2.6), where M243B–Alaska Peninsula had the highest mortality of surveyed forest and shrubland (0.45 percent), followed by 133A–Cook Inlet Basin (0.22 percent) and M133B–Alaska Range (0.19 percent).

A much larger area of Alaska was affected by defoliation than by mortality in 2019. Specifically, nine defoliation agents were found together to affect approximately 340 000 ha, with the greatest area (154 000 ha) encompassed by hemlock sawfly (*N. tsugae*), 45.4 percent of the total for the State (table 2.5). Surveyors attributed a further 113 000 ha with defoliation to birch leafminer (*Fenusa pusilla*, 33.4 percent), 53 000 ha to aspen leafminer (*Phyllocnistis populiella*, 15.7 percent), and 13 000 to willow leaf blotchminer (*Micrurapteryx salicifoliella*, 3.8 percent).

Defoliation in 2018 was relatively high across east-central and southeastern parts of Alaska (fig. 2.7). The ecoregion section with the highest defoliation was M241D–Alexander Archipelago in the Alaska panhandle, with 3.52 percent of surveyed area experiencing defoliation from hemlock sawfly in western hemlock (*Tsuga heterophylla*) forests. Meanwhile, birch leafminer resulted in 2.47- and 1.24-percent defoliation in surveyed forest and shrubland areas of 133A–Cook Inlet Basin and M241C–Chugach-St. Elias

Mountains, respectively, in south-central Alaska. Aspen leafminer and willow leaf blotchminer were the main defoliation agents in ecoregion sections of east-central Alaska: M132C–Yukon-Tanana Uplands (1.03 percent defoliation), 132C–Tanana-Kuskokwim Lowlands (0.87 percent), 132A–Yukon-Old Crow Basin (0.77 percent), and M132E–Ray Mountains (0.64 percent).

Finally, surveyors delineated about 27 000 ha with mortality in Hawaii during 2019 (table 2.3). While no cause was assigned to any of the mortality, at least some of this was likely caused by rapid ‘ōhi‘a death, a wilt disease that affects ‘ōhi‘a lehua (*Metrosideros polymorpha*), a highly ecologically and culturally important tree in Hawaiian native forests (University of Hawai‘i 2020). Rapid ‘ōhi‘a death is caused by the fungal pathogens *Ceratocystis lukuohia* and *C. huliohia*, but *C. lukuohia* is more aggressive than *C. huliohia*, though both can kill ‘ōhi‘a (Barnes and others 2018). Both pathogens have been confirmed extensively on the islands of Hawai‘i (the Big Island) and Kaua‘i, while in 2019 five trees and one tree infected with *C. huliohia* were detected on O‘ahu and Maui, respectively (University of Hawai‘i 2020).

Montane wet ecoregions across the islands of Maui, Hawai‘i, and Molokai were those with the highest mortality detected in 2019 (fig. 2.8): Montane Wet-Maui-East (MWm-e) with 4.00 percent of the surveyed tree canopy area, Montane Wet-Maui-West (MWm-w) with 1.36 percent, Montane Wet-Hawai‘i-Kohala-Hāmākua (MWh-kh) with 1.14 percent,

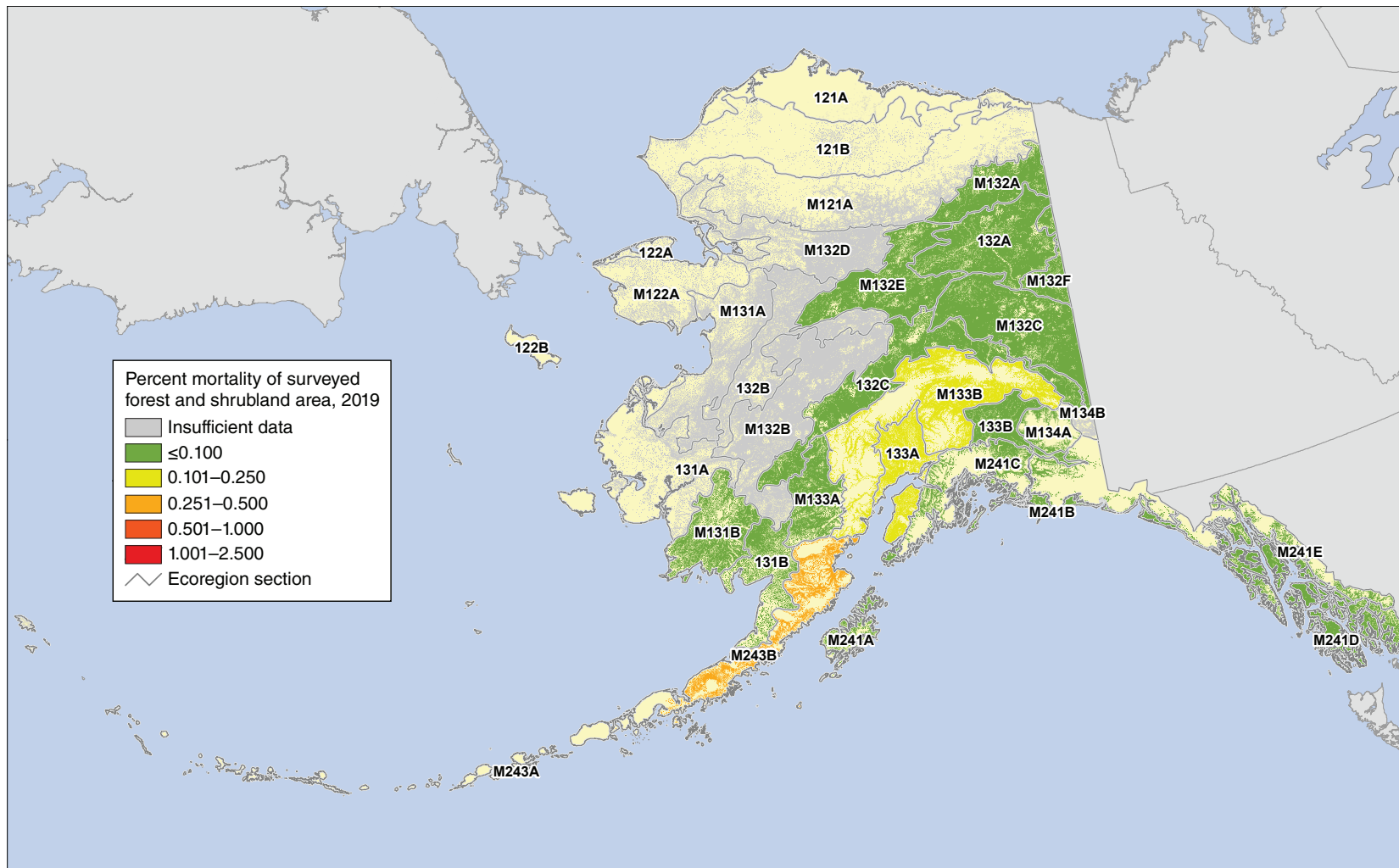


Figure 2.6—Percentage of 2019 surveyed Alaska forest and shrubland area within ecoregions with mortality caused by insects and diseases. The gray lines delineate ecoregion sections (Spencer and others 2002). Forest and shrub cover is derived from the 2011 National Land Cover Database. (Data source: U.S. Department of Agriculture Forest Service, Forest Health Protection)

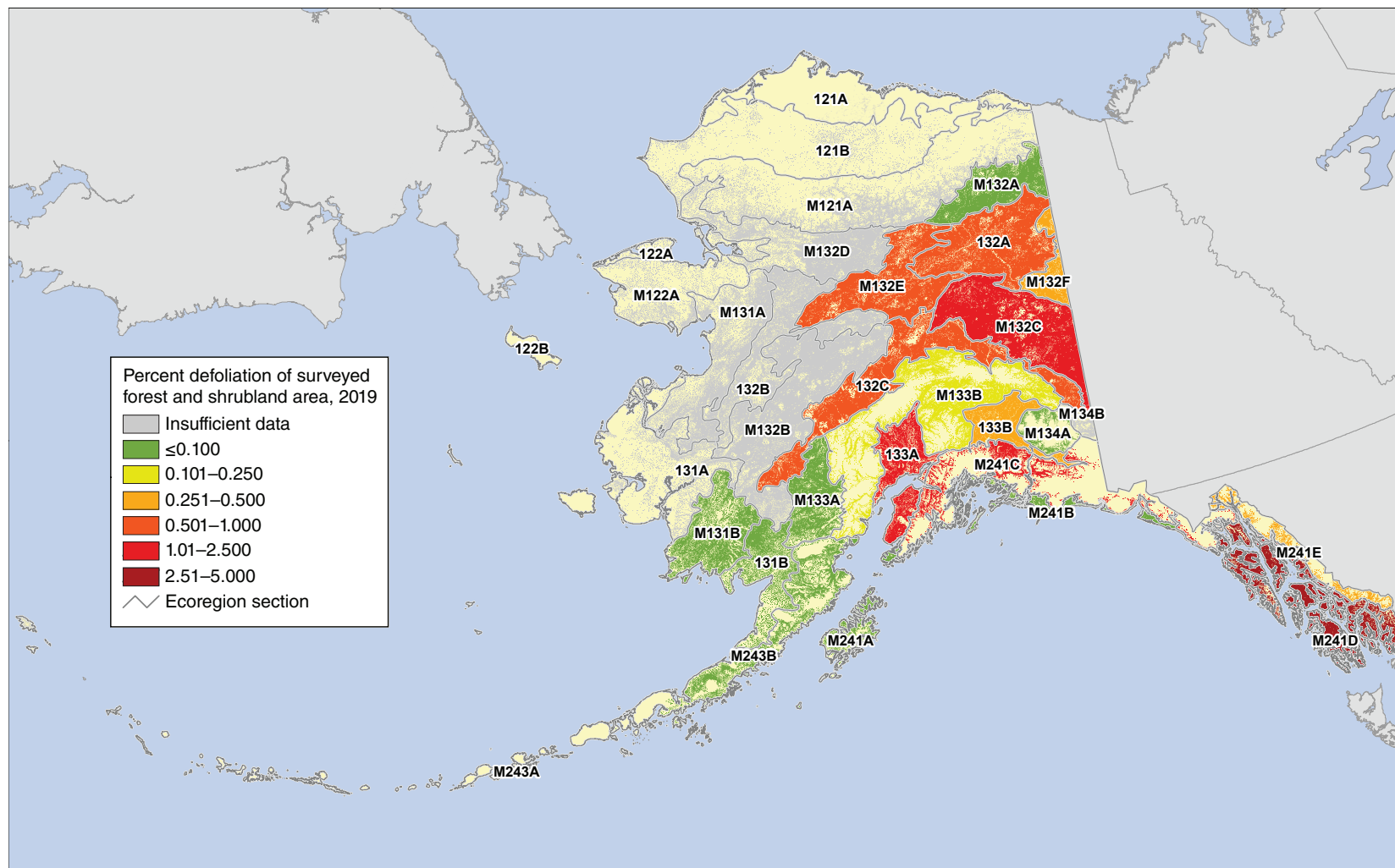


Figure 2.7—Percentage of 2019 surveyed Alaska forest and shrubland area within ecoregions with defoliation caused by insects and diseases. The gray lines delineate ecoregion sections (Spencer and others 2002). Forest and shrub cover is derived from the 2011 National Land Cover Database. (Data source: U.S. Department of Agriculture Forest Service, Forest Health Protection)

Montane Wet-Hawai‘i-Kona (MWh-ko) with 0.94 percent, Montane Wet-Moloka‘i (MWmo) with 0.71 percent, and Montane Wet-Hawai‘i-Ka‘ū (MWh-ka) with 0.69 percent. One lowland wet ecoregion (Lowland Wet-O‘ahu [LWo], 0.70 percent) and one mesic ecoregion (Mesic-Moloka‘i [MEmo], 0.53 percent) also had relatively high levels of mortality. These all were areas with mostly very light to moderate ‘ōhi‘a lehua mortality.

A very small area of Hawaii defoliation (5 ha) was detected in 2019 on O‘ahu, attributed to ‘ōhi‘a/guava rust (*Austropuccinia psidii*) (table 2.5).

CONCLUSION

Continued monitoring of insect and disease outbreaks across the United States will be necessary for determining appropriate followup investigation and management activities. Due to the limitations of survey efforts to detect certain important forest insects and diseases, the pests and pathogens discussed in this chapter do not include all the biotic forest health threats that should be considered when making management decisions and budget allocations. However, large-scale assessments of mortality and defoliation severity offer a useful approach for identifying geographic areas where the concentration of monitoring and management activities might be most effective.

LITERATURE CITED

- Anselin, L. 1992. Spatial data analysis with GIS: an introduction to application in the social sciences. Tech. Rep. 92-10. Santa Barbara, CA: University of California, National Center for Geographic Information and Analysis. 53 p.
- Barnes, I.; Fourie, A.; Wingfield, M.J. [and others]. 2018. New *Ceratocystis* species associated with rapid death of *Metrosideros polymorpha* in Hawaii. *Persoonia-Molecular Phylogeny and Evolution of Fungi*. 40(1): 154–181. <https://doi.org/10.3767/persoonia.2018.40.07>.
- Berryman, E.; McMahan, A. 2019. Using tree canopy cover data to help estimate acres of damage. In: Potter, K.M.; Conkling, B.L., eds. *Forest Health Monitoring: national status, trends, and analysis 2018*. Gen. Tech. Rep. SRS-239. Asheville, NC: U.S. Department of Agriculture Forest Service, Southern Research Station: 125–141.
- Brockerhoff, E.G.; Liebhold, A.M.; Jactel, H. 2006. The ecology of forest insect invasions and advances in their management. *Canadian Journal of Forest Research*. 36(2): 263–268. <https://doi.org/10.1139/x06-013>.
- Castello, J.D.; Leopold, D.J.; Smallidge, P.J. 1995. Pathogens, patterns, and processes in forest ecosystems. *BioScience*. 45(1): 16–24. <https://doi.org/10.2307/1312531>.
- Cleland, D.T.; Freeouf, J.A.; Keys, J.E. [and others]. 2007. Ecological subregions: sections and subsections for the conterminous United States. Gen. Tech. Rep. WO-76D. Washington, DC: U.S. Department of Agriculture Forest Service. Map; Sloan, A.M., cartographer; presentation scale 1:3,500,000; colored. Also on CD-ROM as a GIS coverage in ArcINFO format or at <http://data.fs.usda.gov/geodata/edw/datasets.php>. [Date accessed: July 20, 2015].
- Coleman, T.W.; Graves, A.D.; Heath, Z. [and others]. 2018. Accuracy of aerial detection surveys for mapping insect and disease disturbances in the United States. *Forest Ecology and Management*. 430: 321–336. <https://doi.org/10.1016/j.foreco.2018.08.020>.
- Coulston, J.W.; Moisen, G.G.; Wilson, B.T. [and others]. 2012. Modeling percent tree canopy cover: a pilot study. *Photogrammetric Engineering and Remote Sensing*. 78(7): 715–727. <https://doi.org/10.14358/PERS.78.7.715>.
- Edmonds, R.L.; Agee, J.K.; Gara, R.I. 2011. *Forest health and protection*. Long Grove, IL: Waveland Press, Inc. 667 p.

- ESRI. 2017. ArcMap® 10.5.1. Redlands, CA: Environmental Systems Research Institute.
- Forest Health Protection (FHP). 2019. Digital Mobile Sketch Mapping user's manual 2.1. Fort Collins, CO: U.S. Department of Agriculture Forest Service, Forest Health Assessment and Applied Sciences Team. https://www.fs.fed.us/foresthealth/technology/docs/DMSM_Tutorial/story_content/external_files/DMSM_User_Guide.pdf. [Date accessed: July 10, 2020].
- Forest Health Protection (FHP). 2020. Insect and Disease Detection Survey (IDS) data downloads. Fort Collins, CO: U.S. Department of Agriculture Forest Service, Forest Health Technology Enterprise Team. <https://www.fs.fed.us/foresthealth/applied-sciences/mapping-reporting/detection-surveys.shtml>. [Date accessed: July 6, 2020].
- Getis, A.; Ord, J.K. 1992. The analysis of spatial association by use of distance statistics. *Geographical Analysis*. 24(3): 189–206. <https://doi.org/10.1111/j.1538-4632.1992.tb00261.x>.
- Holdenrieder, O.; Pautasso, M.; Weisberg, P.J.; Lonsdale, D. 2004. Tree diseases and landscape processes: the challenge of landscape pathology. *Trends in Ecology & Evolution*. 19(8): 446–452. <https://doi.org/10.1016/j.tree.2004.06.003>.
- Homer, C.G.; Dewitz, J.A.; Yang, L. [and others]. 2015. Completion of the 2011 National Land Cover Database for the conterminous United States: representing a decade of land cover change information. *Photogrammetric Engineering and Remote Sensing*. 81(5): 345–354.
- Laffan, S.W. 2006. Assessing regional scale weed distributions, with an Australian example using *Nassella trichotoma*. *Weed Research*. 46(3): 194–206. <https://doi.org/10.1111/j.1365-3180.2006.00491.x>.
- Liebhold, A.M.; McCullough, D.G.; Blackburn, L.M. [and others]. 2013. A highly aggregated geographical distribution of forest pest invasions in the USA. *Diversity and Distributions*. 19: 1208–1216. <https://doi.org/10.1111/ddi.12112>.
- Logan, J.A.; Regniere, J.; Powell, J.A. 2003. Assessing the impacts of global warming on forest pest dynamics. *Frontiers in Ecology and the Environment*. 1: 130–137. [https://doi.org/10.1890/1540-9295\(2003\)001\[0130:ATIOGW\]2.0.CO;2](https://doi.org/10.1890/1540-9295(2003)001[0130:ATIOGW]2.0.CO;2).
- Lovett, G.M.; Weiss, M.; Liebhold, A.M. [and others]. 2016. Nonnative forest insects and pathogens in the United States: impacts and policy options. *Ecological Applications*. 26: 1437–1455. <https://doi.org/10.1890/15-1176>.
- Mack, R.N.; Simberloff, D.; Lonsdale, W.M. [and others]. 2000. Biotic invasions: causes, epidemiology, global consequences, and control. *Ecological Applications*. 10(3): 689–710. [https://doi.org/10.1890/1051-0761\(2000\)010\[0689:BICEGC\]2.0.CO;2](https://doi.org/10.1890/1051-0761(2000)010[0689:BICEGC]2.0.CO;2).
- Manion, P.D. 2003. Evolution of concepts in forest pathology. *Phytopathology*. 93: 1052–1055. <https://doi.org/10.1094/PHYTO.2003.93.8.1052>.
- Parry, D.; Teale, S.A. 2011. Alien invasions: the effects of introduced species on forest structure and function. In: Castello, J.D.; Teale, S.A., eds. *Forest health: an integrated perspective*. New York: Cambridge University Press: 115–162. <https://doi.org/10.1017/CBO9780511974977.006>.
- Potter, K.M. 2012. Large-scale patterns of insect and disease activity in the conterminous United States and Alaska from the national Insect and Disease Detection Survey database, 2007 and 2008. In: Potter, K.M.; Conkling, B.L., eds. *Forest Health Monitoring 2009 national technical report*. Gen. Tech. Rep. SRS-167. Asheville, NC: U.S. Department of Agriculture Forest Service, Southern Research Station: 63–78.
- Potter, K.M. 2013. Large-scale patterns of insect and disease activity in the conterminous United States and Alaska from the national Insect and Disease Detection Survey, 2009. In: Potter, K.M.; Conkling, B.L., eds. *Forest Health Monitoring: national status, trends, and analysis 2010*. Gen. Tech. Rep. SRS-176. Asheville, NC: U.S. Department of Agriculture Forest Service, Southern Research Station: 15–29.
- Potter, K.M. 2020. Introduction. In: Potter, K.M.; Conkling, B.L., eds. *Forest Health Monitoring: national status, trends, and analysis 2019*. Gen. Tech. Rep. SRS-250. Asheville, NC: U.S. Department of Agriculture Forest Service, Southern Research Station: 5–24.
- Potter, K.M., Canavin, J.C.; Koch, F.H. 2020a. A forest health retrospective: national and regional results from 20 years of Insect and Disease Survey data. In: Potter, K.M.; Conkling, B.L., eds. *Forest Health Monitoring: national status, trends, and analysis 2019*. Gen. Tech. Rep. SRS-250. Asheville, NC: U.S. Department of Agriculture Forest Service, Southern Research Station: 125–149.

- Potter, K.M.; Escanferla, M.E.; Jetton, R.M.; Man, G. 2019a. Important insect and disease threats to United States tree species and geographic patterns of their potential impacts. *Forests*. 10(4): 304. <https://doi.org/10.3390/f10040304>.
- Potter, K.M.; Escanferla, M.E.; Jetton, R.M. [and others]. 2019b. Prioritizing the conservation needs of United States tree species: evaluating vulnerability to forest insect and disease threats. *Global Ecology and Conservation*. 18: e00622. <https://doi.org/10.1016/j.gecco.2019.e00622>.
- Potter, K.M.; Koch, F.H. 2012. Large-scale patterns of insect and disease activity in the conterminous United States and Alaska, 2006. In: Potter, K.M.; Conkling, B.L., eds. *Forest Health Monitoring 2008 national technical report*. Gen. Tech. Rep. SRS-158. Asheville, NC: U.S. Department of Agriculture Forest Service, Southern Research Station: 63–72.
- Potter, K.M.; Koch, F.H.; Oswalt, C.M.; Iannone, B.V. 2016. Data, data everywhere: detecting spatial patterns in fine-scale ecological information collected across a continent. *Landscape Ecology*. 31: 67–84. <https://doi.org/10.1007/s10980-015-0295-0>.
- Potter, K.M.; Paschke, J.L. 2013. Large-scale patterns of insect and disease activity in the conterminous United States and Alaska from the national Insect and Disease Detection Survey database, 2010. In: Potter, K.M.; Conkling, B.L., eds. *Forest Health Monitoring: national status, trends, and analysis 2011*. Gen. Tech. Rep. SRS-185. Asheville, NC: U.S. Department of Agriculture Forest Service, Southern Research Station: 15–28.
- Potter, K.M.; Paschke, J.L. 2014. Large-scale patterns of insect and disease activity in the conterminous United States and Alaska from the national Insect and Disease Survey database, 2011. In: Potter, K.M.; Conkling, B.L., eds. *Forest Health Monitoring: national status, trends, and analysis 2012*. Gen. Tech. Rep. SRS-198. Asheville, NC: U.S. Department of Agriculture Forest Service, Southern Research Station: 19–34.
- Potter, K.M.; Paschke, J.L. 2015a. Large-scale patterns of insect and disease activity in the conterminous United States and Alaska from the national Insect and Disease Survey, 2012. In: Potter, K.M.; Conkling, B.L., eds. *Forest Health Monitoring: national status, trends, and analysis 2013*. Gen. Tech. Rep. SRS-207. Asheville, NC: U.S. Department of Agriculture Forest Service, Southern Research Station: 19–36.
- Potter, K.M.; Paschke, J.L. 2015b. Large-scale patterns of insect and disease activity in the conterminous United States, Alaska, and Hawaii from the national Insect and Disease Survey, 2013. In: Potter, K.M.; Conkling, B.L., eds. *Forest Health Monitoring: national status, trends, and analysis 2014*. Gen. Tech. Rep. SRS-209. Asheville, NC: U.S. Department of Agriculture Forest Service, Southern Research Station: 19–38.
- Potter, K.M.; Paschke, J.L. 2016. Large-scale patterns of insect and disease activity in the conterminous United States and Alaska from the national Insect and Disease Survey, 2014. In: Potter, K.M.; Conkling, B.L., eds. *Forest Health Monitoring: national status, trends, and analysis 2015*. Gen. Tech. Rep. SRS-213. Asheville, NC: U.S. Department of Agriculture Forest Service, Southern Research Station: 21–40.
- Potter, K.M.; Paschke, J.L. 2017. Large-scale patterns of insect and disease activity in the conterminous United States and Alaska from the national Insect and Disease Survey, 2015. In: Potter, K.M.; Conkling, B.L., eds. *Forest Health Monitoring: national status, trends, and analysis 2016*. Gen. Tech. Rep. SRS-222. Asheville, NC: U.S. Department of Agriculture Forest Service, Southern Research Station: 21–42.
- Potter, K.M., Paschke, J.L.; Koch, F.H.; Berryman, E.M. 2020b. Large-scale patterns of insect and disease activity in the conterminous United States, Alaska, and Hawaii from the national Insect and Disease Survey, 2018. In: Potter, K.M.; Conkling, B.L., eds. *Forest Health Monitoring: national status, trends, and analysis 2019*. Gen. Tech. Rep. SRS-250. Asheville, NC: U.S. Department of Agriculture Forest Service, Southern Research Station: 27–55.
- Potter, K.M.; Paschke, J.L.; Koch, F.H.; Zweifler, M. 2019c. Large-scale patterns of insect and disease activity in the conterminous United States, Alaska, and Hawaii from the national Insect and Disease Survey, 2017. In: Potter, K.M.; Conkling, B.L., eds. *Forest Health Monitoring: national status, trends, and analysis 2018*. Gen. Tech. Rep. SRS-239. Asheville, NC: U.S. Department of Agriculture Forest Service, Southern Research Station: 21–49.

- Potter, K.M.; Paschke, J.L.; Zweifler, M. 2018. Large-scale patterns of insect and disease activity in the conterminous United States, Alaska, and Hawaii from the national Insect and Disease Survey, 2016. In: Potter, K.M.; Conkling, B.L., eds. *Forest Health Monitoring: national status, trends, and analysis 2017*. Gen. Tech. Rep. SRS-233. Asheville, NC: U.S. Department of Agriculture Forest Service, Southern Research Station: 23–44.
- Reams, G.A.; Smith, W.D.; Hansen, M.H. [and others]. 2005. The Forest Inventory and Analysis sampling frame. In: Bechtold, W.A.; Patterson, P.L., eds. *The enhanced Forest Inventory and Analysis program—national sampling design and estimation procedures*. Gen. Tech. Rep. SRS-80. Asheville, NC: U.S. Department of Agriculture Forest Service, Southern Research Station: 11–26.
- Shima, T.; Sugimoto, S.; Okutomi, M. 2010. Comparison of image alignment on hexagonal and square lattices. In: 2010 IEEE international conference on image processing. [Place of publication unknown]: Institute of Electrical and Electronics Engineers, Inc.: 141–144. <https://doi.org/10.1109/ICIP.2010.5654351>.
- Smith, W.B.; Miles, P.D.; Perry, C.H.; Pugh, S.A. 2009. *Forest resources of the United States, 2007*. Gen. Tech. Rep. WO-78. Washington, DC: U.S. Department of Agriculture Forest Service. 336 p.
- Spencer, P.; Nowacki, G.; Fleming, M. [and others]. 2002. Home is where the habitat is: an ecosystem foundation for wildlife distribution and behavior. *Arctic Research of the United States*. 16: 6–17.
- Teale, S.A.; Castello, J.D. 2011. Regulators and terminators: the importance of biotic factors to a healthy forest. In: Castello, J.D.; Teale, S.A., eds. *Forest health: an integrated perspective*. New York: Cambridge University Press: 81–114. <https://doi.org/10.1017/CBO9780511974977.005>.
- Tobin, P.C. 2015. Ecological consequences of pathogen and insect invasions. *Current Forestry Reports*. 1: 25–32. <https://doi.org/10.1007/s40725-015-0008-6>.
- University of Hawai'i, College of Tropical Agriculture and Human Resources. 2020. Rapid 'ōhi'a death. <http://rapidohiadeath.org>. [Date accessed: September 4, 2020].
- U.S. Department of Agriculture (USDA) Forest Service. 2008. National forest type data development. http://svinetfc4.fs.fed.us/rastergateway/forest_type/. [Date accessed: May 13, 2008].
- White, D.; Kimerling, A.J.; Overton, W.S. 1992. Cartographic and geometric components of a global sampling design for environmental monitoring. *Cartography and Geographic Information Systems*. 19(1): 5–22. <https://doi.org/10.1559/152304092783786636>.
- Zhang, L.; Rubin, B.D.; Manion, P.D. 2011. Mortality: the essence of a healthy forest. In: Castello, J.D.; Teale, S.A., eds. *Forest health: an integrated perspective*. New York: Cambridge University Press: 17–49. <https://doi.org/10.1017/CBO9780511974977.003>.